Photometry of the Oort Cloud comet C/2009 P1(Garradd): pre-perihelion observations at 5.7 and 2.5 AU

Photometryof the Oort Cloud comet C/2009 P1(Garradd): pre-perihelion observations at 5.7and 2.5AU

E. Mazzotta Epifani, C. Snodgrass, D. Perna, M. Dall'Ora, P. Palumbo, V. Della Corte, A. Alvarez-Candal, M. Melita, A Rotundi

www.elsevier.com

PII: S0032-0633(15)30060-X
DOI: http://dx.doi.org/10.1016/j.pss.2016.07.007
Reference: PSS4207

To appear in: *Planetary and Space Science*

Received date: 9 October 2015
Accepted date: 10 July 2016

Cite this article as: E. Mazzotta Epifani, C. Snodgrass, D. Perna, M. Dall'Ora, P Palumbo, V. Della Corte, A. Alvarez-Candal, M. Melita and A Rotundi, Photometryof the Oort Cloud comet C/2009 P1(Garradd): pre-perihelio observations at 5.7and 2.5AU, *Planetary and Space Science* http://dx.doi.org/10.1016/j.pss.2016.07.007

Photometry of the Oort Cloud comet C/2009 P1 (Garradd): pre-perihelion observations at 5.7 and 2.5 AU[☆]

E. Mazzotta Epifani[1*], C. Snodgrass[2], D. Perna[2], M. Dall'Ora[4], P. Palumbo[5,6], V. Della Corte[6], A. Alvarez-Candal[7], M. Melita[8], A. Rotundi[5,6]

[1]INAF - Osservatorio Astronomico di Roma, Via Frascati 33, 00078 Monte Porzio Catone (RM), Italy
[2]Dept. of Physical Sciences, The Open University, Walton Hall, Milton Keynes, Buckinghamshire, UK
[3]LESIA, Observatoire de Paris, PSL Reserach University, CNRS, Sorbonne Universités, UPMC Univ. Paris Diderot, Sorbonne Paris Cité, 5 place Jules Jansson, 92195 Meudon, France
[4]INAF - Osservatorio Astronomico di Capodimonte, Via Moiariello 16, 80131 Napoli, Italy
[5]Università Parthenope, DIST, Centro Direzionale Isola C4, 80143 Napoli, Italy
[6]INAF - Istituto di Astrofisica e Planetologia Spaziale, Via del Fosso del Cavaliere 100, 00133 Roma, Italy
[7]Observatório Nacional, Rua General José Cristino 77, 20921-400, Rio de Janeiro, Brazil
[8]IAFE - Universidad de Buenos Aires, Ciudad Universitaria, Intendente Guiraldes s/n, Buenos Aires, Argentina

[*]Corresponding author: elena.epifani@oa-roma.inaf.it

Abstract

The aim of this paper is to contribute to the characterization of the general properties of the Long Period Comets (LPCs) family, and in particular to report on the dust environment of comet C/2009 P1 (Garradd).

The comet was observed at two epochs pre-perihelion, at ~ 6 AU and at ~ 2.5 AU: broad-band images have been used to investigate its coma morphology and properties and to model the dust production rate.

Comet C/2009 P1 (Garradd) is one of the most active and "dust producing" LPCs ever observed, even at the large heliocentric distance r_h ~ 6 AU. Its coma presents a complex morphology, with subtle structures underlying the classical fan-shaped tail, and, at r_h ~2.5 AU, also jet-like structures and spiralling outflows. In the reference aperture of radius $\rho = 5 \times 10^4$ km, the R-Afρ is 3693 ± 156 cm and 6368 ± 412 cm, in August 2010 (r_h ~6 AU) and July 2011 (r_h ~2.5 AU), respectively. The application of a first order photometric model, under realistic assumptions on grain geometric albedo, power-law dust size distribution, phase darkening function and grain dust outflow velocity, yielded a measure of the dust production rate for the two epochs of observation of $Q_d = 7.27 \times 10^2$ kg/s and $Q_d = 1.37 \times 10^3$ kg/s, respectively, for a reference outflow dust velocity of v_{small} = 25 m/s for small (0.1 – 10 μm) grains and v_{large} = 1 m/s for large (10 μm – 1 cm) grains.

These results suggest that comet Garradd is one of the most active minor bodies observed in recent years, highly contributing to the continuous replenishment of the Interplanetary Dust Complex also in the outer Solar System, and pose important constraints on the mechanism(s) driving the cometary activity at large heliocentric distances.

Keywords

Comets, dust; comets, coma

[☆]Based on observations collected at the Italian Telescopio Nazionale Galileo (TNG), operated on the island of La Palma by the Centro Galileo Galilei of the INAF (Istituto Nazionale di Astrofisica) at the Spanish Observatorio del Roque de los Muchachos of the Instituto de Astrof´ısica de Canarias, and on observations collected at the European Organisation for Astronomical Research in the Southern Hemisphere, Chile, with the MPI telescope, proposal 085.C-0324(A).

1 Introduction

The classical vision of the cold and far regions of the outer Solar System is that of the Oort Cloud formed (at least in part) by comets accreted in the Sun's protoplanetary disk, among or slightly beyond the giant planets (r_h ~ 5-30 AU) and then scattered outward (Duncan et al. 1987; Dones et al. 2004). Moreover, recent simulations of cometary origins (Levison et al. 2010) suggest that, the Oort Cloud being much more populous than the models predict, the majority of the comets in this reservoir have an extrasolar origin (likely, captured from protoplanetary disks of other stars). Therefore, the observation of a comet coming directly from the most remote region of our Solar System, as the Oort Cloud is, gives the intriguing opportunity to investigate the characteristics of one of the most primordial witnesses of the early phases of the Solar System.

Comet C/2009 P1 (Garradd) (hereafter comet Garradd) was discovered by G.J. Garradd on 2009 August 13, when it was at a heliocentric distance of r_h = 8.7 AU. Its present orbital parameters are listed in Table 1. Dynamical computations show that Garradd is a hyperbolic comet, with an original reciprocal semi-major axis of +0.000408 AU^{-1} (S. Nakano Note, NK2367, www.oaa.gr.jp/~oaacs/nk/nk2367.htm). Garradd is classified as a (returning) Nearly Isotropic Comet from the Oort Cloud reservoir.

Table 1 - Orbital parameters of the hyperbolic comet C/2009 P1 (Garradd)

a [AU]	E	q [AU]	t_p [yr]	i [°]	Peri [°]	Node [°]
-6285.8	1.000	1.551	23 Dec 2011	106.17	90.72	326.0

a: semi-major axis; e: orbital eccentricity; q: perihelion distance; t_p: time of perihelion passage; i: orbital inclination; Peri: J2000 argument of perihelion; Node: J2000 longitude of the ascending node

Comet Garradd is presently (as per October 2015) very far on its outbound orbital branch after the close perihelion passage in December 2011 at 1.55 AU. It has been a bright comet, which reached visual magnitude V = 6 around perihelion (e.g., Bodewits et al. (2012); see also www.aerith.net/comet/catalog/2009P1/2009P1.html), and was well observable over a wide range of heliocentric distances. It has been the first comet for which the production rate and behaviour of the three main volatiles (H_2O, CO and CO_2) have been measured along a significant part of its orbit in the inner part of the Solar System (Paganini et al. 2012; Villanueva et al. 2012; Combi et al. 2013; DiSanti et al. 2014; Feaga et al. 2014; Bodewits et al. 2014). The Garradd's H_2O outgassing trend showed an increase and a pre-perihelion peak, and then a steady decrease (Feaga et al. 2014; Bodewits et al. 2014), which is a quite comet-typical figure, with a noticeable elevated peak of production rate pre-perihelion in November 2011, consistent with water production rate from icy particles in the coma rather than from direct sublimation from the nucleus (Combi et al. 2013; DiSanti et al. 2014). On the other side, CO outgassing monotonically increased throughout the entire monitored apparition (Feaga et al. 2014), making comet Garradd the comet with the highest CO to H_2O abundance ratio ever observed inside the water snow line (heliocentric distance r < 4-5 AU). Sub-mm observations of the comet from around its perihelion to four months after (Gicquel et al., 2015) depicted Garradd as normal in CH_3OH and depleted in HCN, and confirmed the CO enrichment with respect to typically observed cometary mixing ratio. Also the concentration of C_2, CN, and C_3 molecules and their production rate were studied (Ivanova et al., 2014): it averages 3.3×10^{26} molecules/s, 7.3×10^{26} molecules/s, and 9.7×10^{25} molecules/s, respectively, in the temporal range 28 October – 11 November 2011 (heliocentric distance r = 1.73 – 1.66 AU).

Conversely, the dust environment of comet Garradd has been scarcely investigated during its passage in the Solar System, especially at large heliocentric distances on its inbound orbital branch. Das et al. (2013) and Hadamcik et al. (2014), by means of polarimetric studies of the comet's dust coma 2 months before and after perihelion, depicted a scenario of high dust production rate, with a complex structure of multiple jets and fans. The post-perihelion polarization maps suggested for comet Garradd a classification among the high-P_{max} class of comets, with ejection of small submicron to micron-sized grains, possibly in aggregates.

An estimate of the dust loss rate has been derived from Swift/UVOT V-band phase corrected Afρ from 3.4 AU pre-perihelion (April 2011) to 4 AU post-perihelion (October 2012) by Bodewits et al. (2014). These authors reported that the dust loss rate appeared as distinctly shallower than the gas loss rate, with inferred values of ~ 5×10^3 kgs^{-1} from -250 days (dd) (3.47 AU pre-q) to +150 dd (2.51 AU post-q), with some indications of a dust outburst occurred around 3 AU pre-q (June 2011). Their values of Q_d were derived from the A(0)fρ parameter corrected for the observing heliocentric distance.
From their (and by other authors) long term monitoring of the water production rate of the comet, Bodewits et al (2014) inferred a near constant (minimum) active area of approximately 75 km^2, which, coupled with the estimate of the nucleus upper limit radius of 5.6 km derived by means of standard thermal modeling of mm observations by Boissier et al (2013), results in a continuous active surface fraction of >20% (interestingly, Boissier et al. (2013) derived an even larger surface fraction of at least 50% for comet Garradd, further confirming that this comet is a very active one).
During an observation campaign devoted at investigating the dusty environment of distant new comets, possibly along their inbound orbital branch, we also targeted comet Garradd when approaching the Sun at ~2.5 AU, in July 2011. Images of the comet were obtained at the 3.52-m Telescopio Nazionale Galileo (TNG) at the Observatorio del Roque de los Muchachos (La Palma, Canary Islands). Given the remarkable activity shown by comet Garradd at the time of and after our TNG observations, we searched telescope archives to check if previous pre-q images could be useful in order to better characterize its distant dusty environment. We found multicolour images of comet Garradd in the ESO archives, obtained when it was at 5.7 AU pre-q (August 2010) with the 2.2-m MPG/ESO telescope at La Silla.
In this paper we present our analysis of the pre-q dust environment of the comet, both outside and inside the "snow line" in the Solar System. We describe our data analysis in Section 2 and present our results in Section 3. In Section 4 we use our results, together with results published so far, to model the dust production rate of comet Garradd. Summary and conclusion are given in Section 5.

2 Observations and Data Reduction

2.1 MPG ESO observations

Archive observation of comet Garradd were found, obtained at the 2.2 m ESO/MPG telescope at La Silla (Chile), during an observation run in the night of 2010 August 16. The details of images used in the present analysis are given in Table 2. The observing circumstances for the night are presented in Table 3.
The images were obtained with the WFI (Wide Field Imager) instrument, a focal reducer-type camera at the Cassegrain focus, equipped with a 4x2 mosaic of 2kx4k CCDs for a total field of view of 34'x33', with a scale of 0.238 arcsec/px. The instrument was equipped with the (permanently mounted) broadband filters V (BB#V/89 ESO843), Rc (BB#Rc/162 ESO844), and Ic (BB#I/203 ESO879).
(In the following, the filters are called V, R, and I, respectively, in order to perform a straightforward comparison with the very similar filters (in CW and FWHM) adopted at the other telescope – see below)

2.2 TNG La Palma observations

Comet Garradd has been observed at the 3.52 m Telescopio Nazionale Galileo (TNG) at the Observatorio del Roque de los Muchachos (La Palma, Canary Islands), during an observation run in the night of 2011 July 28. The details of the images obtained during the run and used in the present analysis are given in Table 2. The observing circumstances for the night are presented in Table 3.
The images were obtained with the DOLORES (Device Optimised for the LOw RESolution) instrument, a focal reducer instrument installed at the Nasmyth B focus of the TNG. The detector is a 2048 × 2048 E2V 4240 thinned back-illuminated, deep-depleted, Astro-BB coated CCD with a pixel size of 13.5 μm. The scale is 0.252 arcsec/px, which yields a field of view of about 8.6 × 8.6 arcmin. The instrument was equipped with the broadband filters V, R and I of the Johnson-Cousins system.

Table 2 - Details of the observing sequences on comet C/2009 P1 (Garradd)

Telescope	Filter	Imaging sequences [(a)]	Median airmass
ESO	V	2 × 180	1.134
	R	4 × 180	1.277
	I	4 × 180	1.322
TNG	V	6 × 20	1.115
	R	2 × 20	1.119
	I	1 × 10	1.125

(a) For each filter, the number of image × the exposure time in sec. is given

Table 3 - Observing circumstances of comet C/2009 P1 (Garradd)

Telescope	Obs. time [(a)]	r [AU]	Δ [AU]	α [°]	PsAng [°]	PsAMV [°]
ESO	2010 Aug. 16 00:52	5.73	4.87	5.53	307.7	135
TNG	2011 Jul. 29 00:51	2.48	1.58	13.7	211.7	154

[(a)] UT time at the beginning of the imaging sequence

r: heliocentric distance; Δ: geocentric distance; a: phase angle; PsAng: position angle of the extended Sun-target radius vector; PsAMV: negative of the target's heliocentric velocity vector

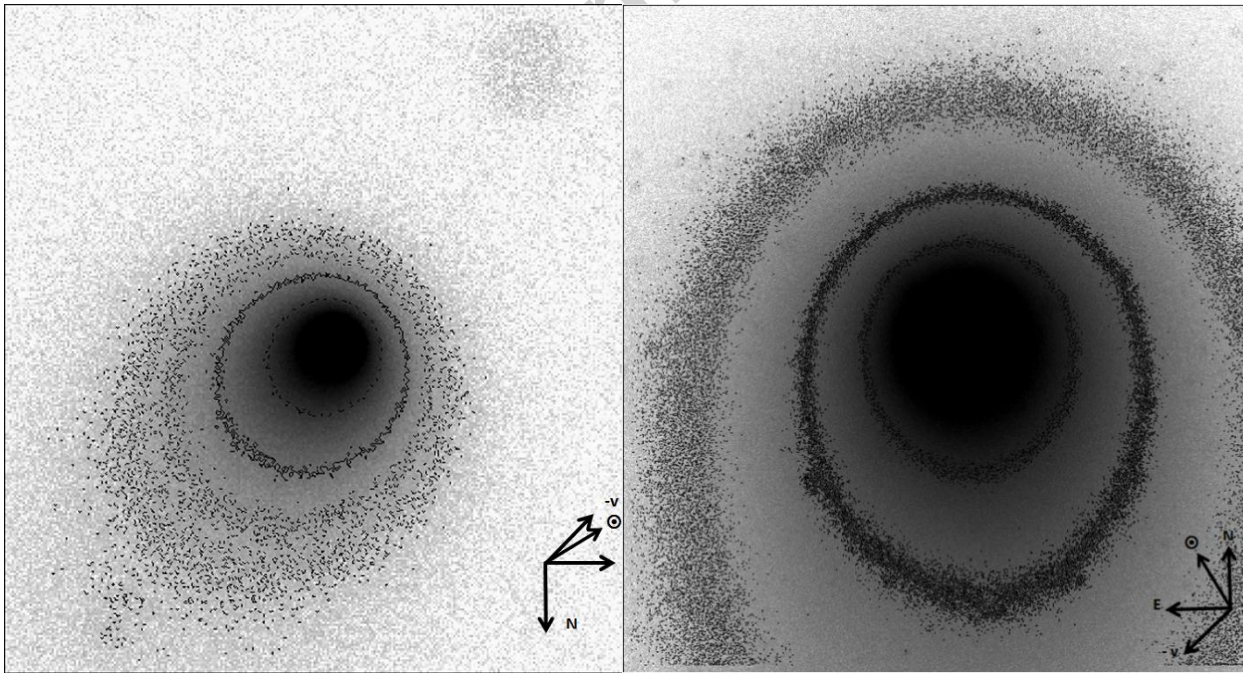

Figure 1 -ESO (August 2010, left) and TNG (July 2011, right) images of comet C/2009 P1 (Garradd) in the R filter. The linear scale is 2.3×10^5 km and 2.5×10^5 km, respectively. N, E, Sun direction, and velocity vector are indicated. The faintest contour corresponds to 23.23 R_{mag}/arscec^2 and 23.20 R_{mag}/arcsec^2, for the two epochs, respectively. The look-up table is neglog, black represents higher brightness intensity.

2.3 Data Reduction

During both observing nights, several short (or very short, in case of TNG observations) exposures were obtained for the target, the telescope tracking at the non-sidereal rate corresponding to the predicted motion of the comet. All the images were corrected for overscan, bias, and flat-fielding in the standard manner, using tools available in IRAF and ESO's MIDAS (Munich Image Data Analysis System): the bias value was obtained from an average of several zero-exposure frames, taken at the beginning of each night, while a masterflat for each filter was obtained by averaging several twilight exposures (individually corrected for bias).
In order to increase the SNR and to remove or at least reduce any residual background star contribution, for each filter the images obtained in both runs were accurately inspected (in the framework of the whole observing night) to eventually reject those affected by cirrus and clouds. The images selected for the analysis were then (for each filter) median averaged, after recentering them to the comet optocentre found by fitting a two-dimensional Gaussian curve to the innermost pixels of the coma. Then, the sky correction was performed by subtracting a first-order polynomial sky approximation computed from the pixel areas of the same median comet image, both containing no stars and far away from a possible coma contamination.
Figure 1 shows an example of the obtained images, for the R filter, for both the observing runs. The images are shown with very similar linear scale for both the runs, in order to show the changes in the general aspect of the dust coma when comet Garradd moved from 5.7 to 2.5 AU.
Appropriate fields from the list of Landolt (1992) observed at different airmasses during both nights were used to perform an absolute flux calibration of the comet images and obtain quantitative photometric results. The accuracy of the photometric calibration of the data was assured by an independent check, made by means of standard stars of the APASS (AAVSO Photometric All-Sky Survey, see https://www.aavso.org/apass) catalogue, identified in the comet images taken in all the filters.

3 Observational Results

3.1 Coma Morphology

Coma morphology is a powerful tool to investigate the nucleus and coma properties, by observing and interpreting different features such as, e.g., bright jets, fans, and arc structures (Farnham 2009). To investigate the coma images, in order to search for distinct extended features, we applied the so-called radial renormalisation method (Birkle & Boehnhardt 1992), commonly applied to cometary broad-band images (see e.g. Mazzotta Epifani & Palumbo 2011; Mazzotta Epifani et al. 2014a).
For the purpose of the present analysis, we applied it with the following procedure: (1) the mean radial brightness in concentric rings of 1 pixel width was computed around the optocentre of the coma, and used to build an artificial image with the radial dependance of the original one; (2) the original image was divided or subtracted by the mean radial image, to enhance coma magnitude variations relative to the mean radial coma brightness. The radial renormalisation method has been applied to the images obtained in the R filter only, for both the runs. The R filter is the best for an analysis of the dust environment, as it is both the one which presents the highest signal-to-noise ratio in our set of images, and the one least affected by possibly present gaseous emissions (e.g., C_2 and NH_2 lines in the 4000-6000 Å wavelength range). The results are shown in Figures 2 and 3.

3.1.1 Comet Garradd at 5.7 AU pre-q

The general aspect of the coma shows a regular coma, distorted in the anti-solar direction in a tail-like structure. The analysis with the radial renormalisation method (Figure 2) shows a coma characterised by a classical fan-shaped tail extended in the anti-solar direction, with no well-defined deviation either at small or at large scale (such as, e.g., well collimated jets, arcs, fans, and so on). Some subtle shell-like structures appear, enhancing a small brightness excess approximately in the anti-solar direction. We would tend to attribute this effect to dust released in the coma, eventually under the form of short-term, broad "outflows", which then move within the coma as the comet proceeds along its orbit.

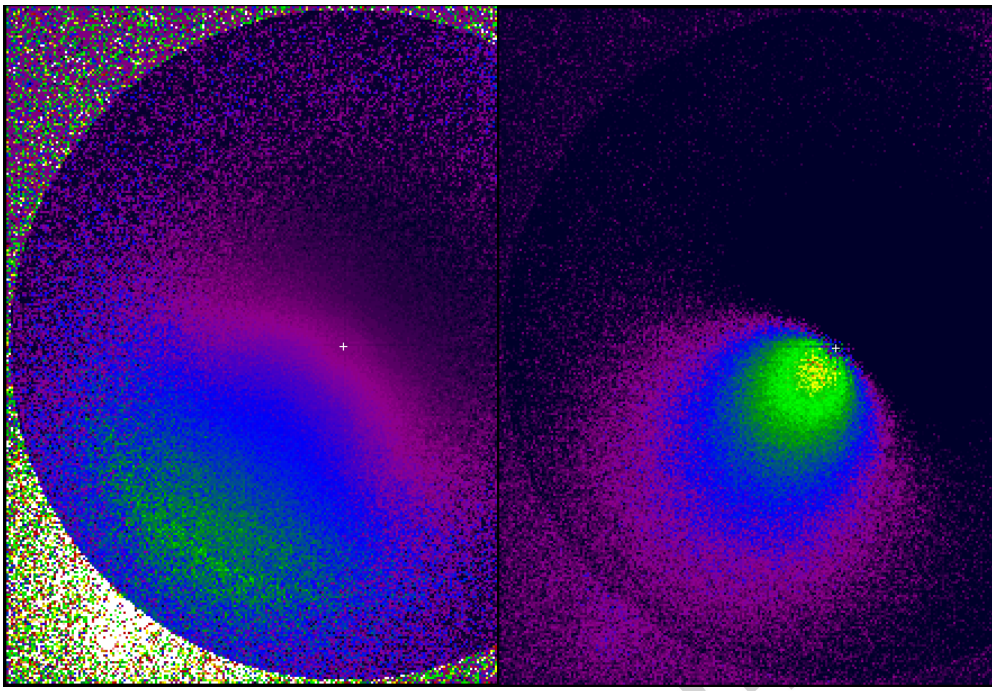

Figure 2 - Morphological analysis of ESO (August 2010) R-filter images of comet C/2009 P1 (Garradd). The linear scale is the same of Figure 1. The white cross indicates the optocenter. (Left) The radial renormalised median-averaged image obtained as quotient of the original image versus the mean radial image. (Right) The radial renormalised median-averaged image obtained as subtraction of the mean radial image from the original image.

Anyway, this effect could also be an artifact resulting from the division of the initial photometric image by the mean radial image, as the division of the initial image by the mean radial image could have artificially enhanced the outer part of the coma (outside ~ 2×10^4 km from the optocentre) in the antisolar direction, due to the corresponding pixels in the solar direction not affected by the coma luminosity. To investigate this issue, we performed also the subtraction of the mean radial image from the initial one (see Figure 2b), and we see that in this case the processed image looks quite a "standard" fan-shaped coma. This would correspond to a nearly isotropic outflow of dust from comet Garradd on August 2010.

3.1.2 Comet Garradd at 2.5 AU pre-q

At the second epoch of observation, comet Garradd also shows an apparently regular dust coma (Figure 1), slightly distorted roughly in the anti-solar direction. Conversely, the renormalisation process (Figure 3) shows a highly complex coma morphology underlying the apparent standard aspect of the coma, even if quite subtle with respect to the latter.

The "dust" R image, in fact, shows a very peculiar behaviour. In our image, the most prominent large-scale feature is a large twisted structure, oriented towards the northern hemisphere, clearly curving clockwise (i.e., towards W), extending at least over a linear scale of 2.5×10^5 km. There is, also, an excess of brightness in the S-S-W direction. This brightness excess is in the same direction, but broader and more distant from the optocenter with respect to a similar excess observable a few days before (Bodewits et al. (2014), their Figure 5).

The complex structures observed in the coma could be considered as hints of nucleus rotational effects in presence of an active area on the surface. A similar twisted structure was observed, e.g., in the dust coma of C/2005 L3 (McNaught) (Mazzotta Epifani et al. 2014a). This effect could be due to the existence of an "active area" (which could mean e.g. a surface portion with different composition or an exposed ice area, eventually exposed to direct solar illumination) that emits a dust and/or gas outflow with a certain repeatability, depending on the nucleus properties. To better explore this aspect, a zoom-in on the dust coma morphology of the innermost coma is shown in Figure 3, right panel. Comet Garradd shows a clearly structured coma morphology, in the vicinity of the nucleus (inner coma: 9 ×

10^4 km), with a faint but still visible multiple jet-like structure extending towards N, clearly evident over a ~10^4 km linear scale. The structure appears to be separated in at least two substructures, whose axes are oriented at 2° and 28° westward from the N, respectively. Moreover, the jet structure appears "disconnected" by the broader curved feature observed in the wider image: this could be due to a possible modulation of the ejection activity from an active area on the nucleus with respect to local illumination condition.

3.2 Coma Photometry and Colours

For each epoch of observation, the magnitude values for all the filters have been measured and are summarised (for some selected apertures centred in the comet optocentre) in Table 4. The final uncertainty in the magnitude comes from the calibration error σ_{calib} (rms of the standard stars fit, weighted by the star counts against the background). The magnitude of the comet increased greatly among the two epochs of observations, reaching the remarkable value of ~9 in the visible range in July 2011 (~5 months before perihelion).

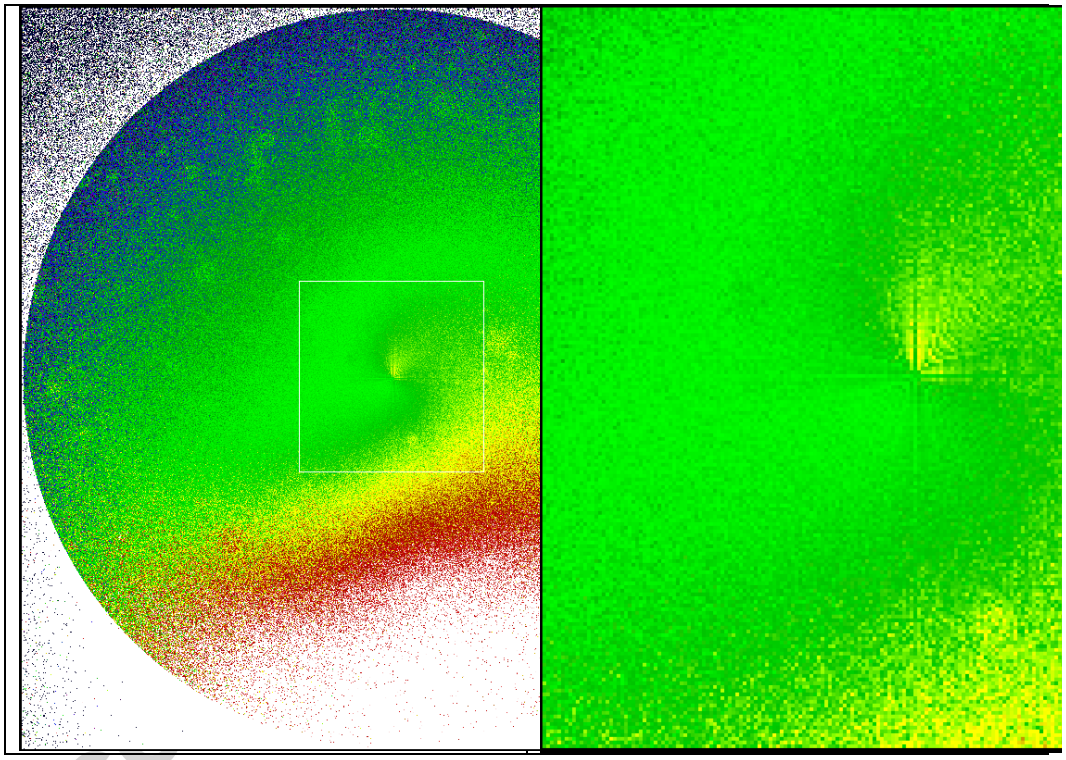

Figure 3 - Morphological analysis of TNG (July 2011) R-filter images of comet C/2009 P1 (Garradd). The radial renormalised median-averaged image is obtained as quotient of the original image versus the mean radial image. (Left) The linear scale is the same of Figure 1. (Right) Innermost part of the comet C/2009 P1 (Garradd)'s coma (linear scale 8.6×10^4 km) for the TNG (July 2011) observation epoch (white box in left panel).

Table 4 - Integrated coma magnitude of comet Garradd, derived for all the filters in selected optical apertures centred on the optocentre, for the two epochs of observation.

$\rho^{(a)}$	Filter	Integrated magnitude$^{(b)}$	
[10^4 km]		August 2010	July 2011
1	V	16.41 ± 0.04	11.43 ± 0.11
	R	15.96 ± 0.05	11.03 ± 0.07
	I	15.50 ± 0.03	10.55 ± 0.10
5	V	14.80 ± 0.04	9.80 ± 0.11
	R	14.34 ± 0.05	9.49 ± 0.07
	I	13.89 ± 0.03	8.96 ± 0.10
8	V	14.57 ± 0.04	9.39 ± 0.11
	R	14.11 ± 0.05	9.12 ± 0.07
	I	13.64 ± 0.03	8.56 ± 0.10

(a) radius of the photometric aperture; (b) uncertainty coming from the calibration error

Table 5 - Colour indexes of comet Garradd, derived in selected optical apertures centred on the optocentre, for the two epochs of observation.

$\rho^{(a)}$	Colour index / Reddening (Colour slope) in %/1000 Å			
	V-R		R-I	
[10^4 km]	August 2010	July 2011	August 2010	July 2011
1	0.46 ± 0.06 / 0.94	0.39 ± 0.13 / 0.35	0.45 ± 0.06 / 0.85	0.87 ± 0.12 / 1.00
5	0.46 ± 0.06 / 0.94	0.32 ± 0.13 / -0.28	0.45 ± 0.05 / 0.83	0.84 ± 0.12 / 1.41
8	0.46 ± 0.06 / 0.97	0.26 ± 0.13 / -0.66	0.47 ± 0.05 / 0.98	0.83 ± 0.12 / 1.76
Solar	0.354		0.332	

$^{(a)}$ radius of the photometric aperture; $^{(b)}$ solar colours in the modern Johnson-Cousins system (Holmberg et al., 2006)

Table 5 summarises the coma colours obtained for some selected reference optical apertures.

In August 2010, the colours of the comet dust appeared quite constant with the increasing aperture, slightly redder than the Sun as often observed for SPCs nuclei (Lamy et al. 2004, 2009; Snodgrass et al. 2005) and similar to what already observed for other Long Period Comets (LPCs) comae (e.g., Mazzotta Epifani et al. (2010), (2014a)) at similar heliocentric distances.

The situation is quite different for the TNG (July 2011) epoch. V-R colour in the vicinity of the nucleus is quite grey with respect to solar colour, becoming slightly bluer (but, admittedly, within the measurement errors) as we move away from the nucleus, towards the external part of the coma. On the contrary, the R-I colour appears slightly red with respect to solar colour.

The interpretation of such a behaviour is not straightforward, and must take into account also the quasi-contemporary observations reported by other authors. For example, Bodewits et al. (2014) reported an evident excess in the Swift/UVOT V-band filter just around the time of our TNG observations (see their Table 1). Bodewits et al. (2014) interpreted this V-band excess as an evidence of an outburst in the water production, likely due to an additional source of water in the coma. This hypothesis was already explored by Combi et al. (2013), which suggested the presence of an "icy halo" in the coma , responsible for water production rather than gas sublimated directly from the nucleus. Analyzing spectroscopic observations of comet Garradd taken at the beginning of September 2011 (only 1 months after our TNG observations), Villanueva et al. (2012) reported an excess of water in the projected sunward direction, probably implying the existence of a "water jet", or an extended source of water.

Therefore, we tend to associate the bluer colour in Garradd's coma (in July 2011) to an outburst in water production, probably due to gas emission in V more than any dust properties (as there are stronger bands in V than in R and I).

3.2.2 Afρ

The Afρ value (expressed in cm), as an estimate of the solar radiation reflected by the cometary dust coma, is almost universally used for the measurement of the cometary dust continuum, as it is considered a proxy for the dust production. It has been introduced by A'Hearn et al. (1984), and recently re-discussed by Fink & Rubin (2012), who analysed the link of the Afρ measurement with dust production rate estimates.
If formulated to take into account the solar flux scattered by the cometary dust towards the observer, the Afρ can be derived from the calculated photometric dust coma magnitude as follows:

$$Af\rho = \frac{4r^2\Delta^2 10^{0.4(m_s - m_c)}}{\rho}$$

where A is the average grain albedo, f the filling factor in the aperture field of view, ρ the linear radius of the aperture at the comet, r the heliocentric distance, Δ the geocentric distance, m_s the Sun magnitude, and m_c the cometary magnitude, measured in the aperture of radius ρ.
The R filter is the more indicated to explore the dust environment of the comet with the Afρ tool, since it is the least affected by gaseous emissions that can strongly influence the comet's luminosity. The R-Afρ values of for comet Garradd, derived in some selected apertures centred on the optocentre, are listed in Table 6, for both the epochs of observations.

Table 6 - R-Afρ values of comet C/2009 P1 (Garradd) for the two epochs of observations

ρ	Afρ [cm]	
[10^4 km]	Aug 2010	Jul 2011
1	4176 ± 176	7642 ± 496
5	3693 ± 156	6368 ± 412
8	2885 ± 122	5535 ± 359

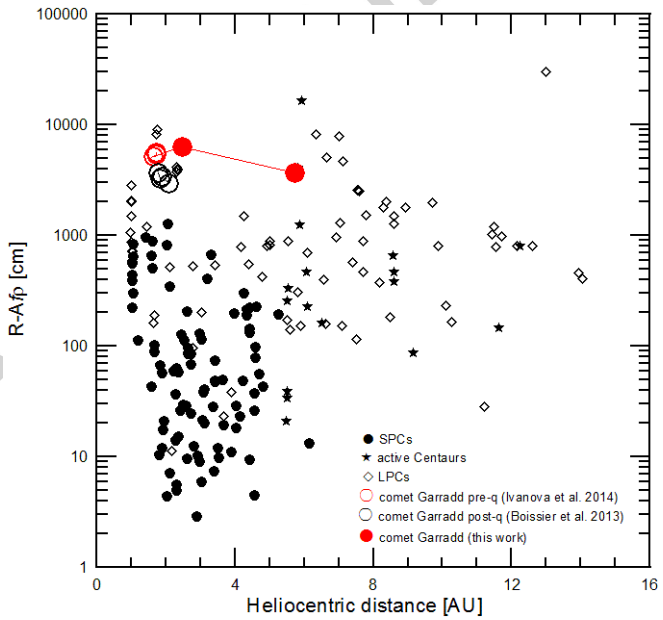

Figure 4 - R-band Afρ values measured for comet Garradd, both pre- and post- perihelion passage (observation period: August 2010 - March 2012), obtained in this work and by Ivanova et al. (2014) and Boissier and al. (2013), compared to values derived for several other minor bodies: SPCs, active Centaurs, and LPCs. Literature was searched for both snapshot and monitoring observations: Mazzotta Epifani & Palumbo (2011), Mazzotta Epifani et al. (2006; 2007; 2008; 2009; 2010; 2011; 2014a; 2014b), Lowry et al. (1999; 2003), Lowry and Fitzsimmons (2001; 2005), Solontoi et al. (2012), Szabó et al.

(2002), Ivanova et al. (2011, 2015), Jewitt (2009), Bauer et al. (2003), Lara et al. (2003), Korsun et al. (2010; 2014), Meech et al. (2009); Shubina et al. (2014).

For both the epochs of observations, the data show that the R-Afρ parameter is not constant vs. the cometocentric aperture, since a monotone decrease in the R-Afρ values with the nucleocentric distance is clearly observable. This effect has been often interpreted as due to a non-steady-state dust emission, and possibly dust grain fading or destruction (Tozzi et al., 2003; Lara et al., 2004).
The R-Afρ parameter is used to compare dust production rate between comets, even if one should keep in mind that it involves several observational and physical parameters, such as the aperture size (if the R-Afρ is not constant with the cometocentric distance), the geometric albedo of the grains, which in turn depends on the observing phase angle, the grain size distribution, and so on. Nevertheless, as a general rule it is assumed that large Afρ values indicate high dust activity.
Figure 4 shows the comparison of R-band Afρ obtained in the reference aperture of $\rho = 5 \times 10^4$ km in the present paper for comet Garradd with the values obtained for several cometary objects (SPCs and LPCs) in the past, from both snapshot and monitoring observations. The values measured for comet Garradd in other epochs of observations (Ivanova et al.,2014; Boissier et al., 2013) are also reported.
It is clearly evident that comet Garradd is one of the most active minor bodies observed in recent years, with Afρ values measured in the period August 2010 - March 2012 around its perihelion passage (in December 2011) much greater than those measured for all the SPCs and for most LPCs at comparable heliocentric distance.

4 Dust Production Rate

The Afρ parameter is considered a good proxy for the measurement of the "dustiness" (and of the degree of activity) of a comet. In fact A'Hearn et al. (1995) quoted (from C. Arpigny, unpublished) an empirical correlation of Afρ parameter with dust production rates Q_d, showing that 1 cm in Afρ corresponds to ~ 1 kg/s of dust production. To obtain a more quantitative measurement of the cometary dust production rates Q_d for comet Garradd, we decided to apply a "photometric model", which relates the optical photometry to the dust production rate via some (as realistic as possible) assumptions on the cometary dust environment.
The method is derived from the one used by Jewitt (2009) to compute the dust production rate of active Centaurs in the region between 5 and 12 AU, and was adapted and already successfully applied by our group to several active minor bodies such as long period comets (Mazzotta Epifani et al. 2010, 2014a), short period comets (Mazzotta Epifani & Palumbo 2011), and active Centaurs (Mazzotta Epifani et al. 2011, 2014b), in a wide range of heliocentric distance. The method is fully described in our papers listed above. Here we recall only that the method consists of relating the total cross-section C_d of the coma dust particles, derived from the photometry in an annular region of the dust coma, to the dust mass M_d of the coma itself, through adopting a power-law dust size distribution. The dust-loss rate Q_d is finally obtained by considering the time of residence of dust grains in the projected coma portion (annulus).
A number of assumptions are made to apply the model for both the observing epochs:
- Geometric albedo A: this is an important factor of uncertainty in our calculations since the actual albedo of dust grains in the coma is unknown. We decided to adopt the typical value of A = 0.04 for comet nuclei, also to be consistent with other studies on Long Period Comets with the same method (Mazzotta Epifani et al., 2014a).
- Phase darkening Φ(α): the shape of this function depends upon a variety of properties of dust particles, including the distribution in size, roughness, and albedo. We adopted the "Schleicher's method" (Schleicher et al. 1998; Schleicher 2007) which is based on the shallower dust comae phase function with respect to that of the bare cometary nucleus. Since comet Garradd was observed at a small phase angle in both epochs (see Table 2), we decided to use the tabulated value of Schleicher's curve normalised at 0◦ (asteroid.lowell.edu/comet/dustphaseHM_table.txt): Φ(α) = 0.7906 and 0.6049, for August 2010 and July 2011, respectively.
- Power-law dust size distribution: numerical modelling of the dust environment for several comets observed by ground (Fulle et al. 1998; Korsun & Chorny 2003; Mazzotta Epifani et al. 2009; Korsun et al. 2010) and analysis of in-situ dust particle cometary environments (Mazets et al., 1986; Price et

al., 2010; Zubko et al., 2015) suggest the adoption of the values of q = -3 for grains in the range 0.1 – 10 μm (hereinafter called small grains) and q = -3.5 for grains between a_- = 10 μm and a_+ = 1 cm (called large grains). Grains are assumed to be compact, with bulk density δ = 1000 kg/m^3. Adopting this value, we are fully consistent with similar analysis of the dust environment of other LPCs (Mazzotta Epifani et al. 2014a).

- Dust outflow velocity v(r) at the heliocentric distance r: this parameter is strictly dependent on dust size, as many numerical simulations of dust coma and tails have shown in the past (see e.g. a summary in Fulle 1999 for Short Period Comets). The grains have been observed to be much slower than the expanding gas in the coma, especially at low (< 3 AU) heliocentric distance. In this work, we adopted a reference value of v_{small} = 25 m/s for small grains and a reference value of v_{large} = 1 m/s for the large grains, for both the observing epochs. These two values are chosen to take into account for the size dependence of the grain velocity, as derived from the dynamical simulation of many comets (e.g., Fulle et al., 1997; Colangeli et al., 1998; Mazzotta Epifani et al., 2009).

To compare results for comet Garradd at both the observing epochs, we decided to select two cometocentric distances in the coma to define the "photometric annulus" used to derive the coma photometry: an inner radius of ρ' = 7535 and 7478 km for the Aug 2010 and Jul 2011 epoch, respectively, and an outer radius of ρ" = 17583 and 17545 km for the Aug 2010 and Jul 2011 epoch, respectively. This annulus has been selected to ensure that any possible nucleus contribution is excluded and the effects of residual sky background are minimised. The linear cometocentric distances of the annulus are selected to be similar for the two observational epochs, to obtain two comparable measurements, but, in the framework of a varying coma like that of comet Garradd, the comparison can be only indicative of the actual cometary activity as a "dust emitter".

Table 7 - Model dust mass-loss rate for comet Garrad for the two epochs of observation.

Observational epoch	m_a [(a)]	C_d [(b)] [m2]	M_d [(c)] [kg]	Q_d [(d)] [kg/s]
Aug2010 (ESO)	15.71	1.32×10^{10}	8.7×10^7; 5.7×10^9	7.27×10^2
Jul2011 (TNG)	11.11	2.35×10^{10}	1.6×10^8; 9.9×10^9	1.37×10^3

(a) Coma magnitude in the selected projected annulus; (b) Derived dust cross section; (c) Derived dust mass in the annulus (the two values are for small and large particles, respectively); (d) Derived dust mass-loss rate for grains crossing the projected coma annulus at the reference velocity values of v_{small} = 25 m/s and v_{large} = 1 m/s (the value is given by the sum of Q_{d_small} + Q_{d_large})

Table 7 summarises, for both the observational epochs, the values derived for all the model quantities and the dust production rate Q_d for the reference velocity of v_{small} = 25 m/s and v_{large} = 1 m/s. Values are actually indicative, as results show that even a small change of v_{large} (e.g., from 1 to 5 m/s) can more than double the resulting Q_d (e.g., from 1.37×10^3 to 5.3×10^3 in July 2011). Nevertheless the behavior of the Q_d obtained by the application of the photometric model clearly shows that Garradd can be considered a strong dust emitter, with the emission of dust increasing with the decrease of the heliocentric distance, as expected, doubling from the value of ~700 kg/s in August 2010 (at r = 5.73 AU) to the value of ~1400 kg/s in July 2011 (at r = 2.48 AU).

5. Discussion and Conclusions

In Figure 5, we decided to compare the range (lower-to-upper limit) of dust production Q_d we found with our method (depending mainly on the high expected variability of the dust outflow velocity, see above) with the dust production measured or derived for other minor bodies: SPCs, active Centaurs and other LPCs.

A direct comparison between Q_d for different comets is not straightforward, as many model and observational factors influence the resulting dust mass-loss rate. Nevertheless, from the general picture it is possible to conclude that comet Garradd is one of the most active dust emitter among the whole

Minor Bodies complex and, in particular, among the LPCs observed in recent years. Incidentally, we note that there is an evident (and surprising) lack of measurements of dust production rate for LPCs at "short" (< 4-5 AU) heliocentric distance, where activity is mainly driven by sublimation of water ice. More measurements in this range close to the Sun would be needed to add points to the plot, to complete the picture of cometary dust release in the inner region of the Solar System.

From the results presented in this paper and already present in literature (see e.g. Figure 4), we can conclude that for comet Garradd the dust production is higher pre-perihelion than post. That is unusual, since most comets show an asymmetry with higher activity after perihelion (e.g. Kelley et al. 2013), which makes more sense in terms of a thermal wave reaching deeper ice after maximum insolation. Combined with the odd pattern in gas emission (CO increasing all the time), the activity pattern of Garradd seems peculiar. One possibility is that Garradd was characterized by the presence of some unusually large amount of near surface volatiles that drove its distant activity, still far from the perihelion passage, but were rapidly depleted before perihelion. Also the presence of gas sublimation (on the inbound leg) from rather big grains close to the nucleus surface could influence the peculiar gas and dust behaviour: the sublimation would in fact stop at a certain point (likely close the perihelion passage) as the near surface ice is gone (and can't be released as grains any more).

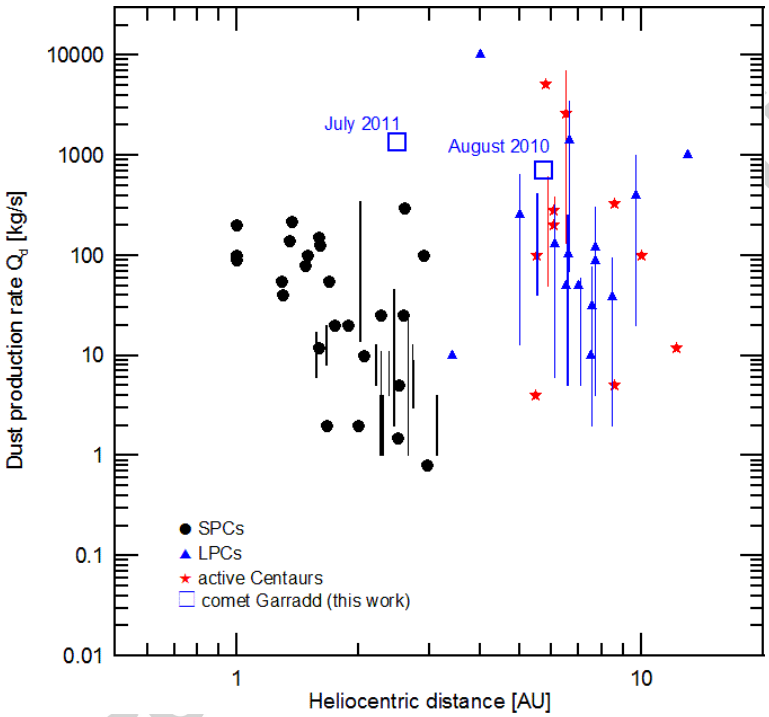

Figure 5 - Dust production rate Q_d of comet Garradd for the two epochs of observations, compared to values derived from literature for several minor bodies: SPCs, active Centaurs, and LPCs. For each group, the vertical lines indicate the min-max range derived for typical/depleted comet classification or range computed by means of the photometric method. References: Mazzotta Epifani et al. (2014a: their Figure 6).

To summarize: we performed multicolor broad-band photometry of the hyperbolic comet C/2009 P1 (Garradd), observed before perihelion, with the 2.2-m MPG/ESO telescope at r_h = 5.7 AU and with the 3.5-m TNG telescope at r_h = 2.5 AU.

Our main results can be summarized as follows:

(1) comet Garradd was very active and "dust producer" already at ~6 AU, with a classical fan-shaped tail extended in the anti-solar direction. Some subtle sub-structures suggest the presence of short-term, broad dust "outflows". When at 2.5 AU, comet Garradd presented a complex coma and tail morphology, with a large twisted structure in the northern hemisphere, curving clockwise, and extending over a linear scale of at least 2.5 × 105 km. In the innermost part of the coma, comet Garradd shows a faint but still visible jet-like structure extending towards N, apparently "disconnected" from the broader large-scale curved feature: this could be due to a possible modulation

of the ejection activity from an active area on the surface, in presence of nucleus rotation and variability of local illumination conditions.

(2) at ~6 AU comet Garradd presented coma colours quite constant with the increasing aperture, slightly redder than the Sun as often observed for other minor bodies: (V-R) = 0.46 ± 0.06 and (R-I) = 0.45 ± 0.05 (in $\rho = 5 \times 10^4$ km). When closer to the Sun, the (V-R) colour of the coma became grey with respect to solar colour ((V-R) = 0.32 ± 0.13), becoming also slightly bluer at longer cometocentric distance, while the (R-I) colour appears quite red with respect to the Sun ((R-I) = 0.84 ± 0.12). This unusual behaviour is interpreted as due to an outburst in water production, probably due to gas emission in V more than any dust properties (as there are stronger bands there than in R and I).

(3) The R-Afρ of comet Garradd, as measured in an aperture of $\rho = 5 \times 10^4$ km, is 3693 ± 156 cm and 6368 ± 412 cm, in August 2010 (r_h ~6 AU) and July 2011 (r_h ~2.5 AU), respectively. These values are much greater than those measured for all the SPCs and for most of the LPCs at comparable heliocentric distances.

(4) the application of a first order photometric model, under realistic assumption on grain geometric albedo and power-law dust size distribution, phase darkening function and grain dust outflow velocity, yielded a measure of the dust production rate Q_d for the two epochs of observation: $Q_d = 7.27 \times 10^2$ kg/s and $Q_d = 1.37 \times 10^3$ kg/s, respectively, for a reference outflow dust velocity of $v_{small} = 25$ m/s for small (0.1 – 10 μm) grains and $v_{large} = 1$ m/s for large (10 μm – 1 cm) grains.

(5) Both the results on R-Afρ and on the derived dust production rate Q_d allow us to derive that comet Garradd is one of the most active minor bodies (in terms of dust emission) ever observed in recent years, similar to the "paradigm" comet C/1995 O1 (Hale-Bopp) (Q_d ~ 500 kg/s at r_h ~ 13 AU, Fulle et al. 1998). This fact, together with its dynamical origin in the Oort cloud and the estimate on its nucleus size, poses interesting constraints on a number of still not entirely explored issues such as the original composition (in terms of solid and volatile compounds) in the extreme region of the Solar System, the mechanism(s) driving the cometary dust emission even at large heliocentric distances, and the contribution of dust loss from LPCs to the replenishment of the Interplanetary Dust Complex and even of the Dust Rings Complexes in the outer Solar System region.

Aknowledgements

CS received funding from the European Union Seventh Framework Program (FP7/2007-2013) under grant agreement no. 268421 and from the UK STFC in the form of as Rutherford fellowship.
AAC acknowledges funding from CNPq.

References

- A'Hearn M.F., Schleicher D.G., Feldman P.D., Millis R.L. & Thompson D.T., 1984, AJ 89, 579
- A'Hearn M.F., Millis R.C., Schleicher D.O., Osip D.J. & Birch P.V., 1995, Icarus 118, 223
- Bauer J.M., Fernandez Y.R., Meech K.J., 2003, PASP 115, 981
- Birkle K. and Boehnhardt H., 1992, EM&P 57, 191
- Bodewits D., Farnham T. & A'Hearn M.F., 2012, CBET 3090
- Bodewits D., Farnham T.L., A'Hearn M.F. et al., 2014, ApJ 786, 48
- Boissier J., Bockel´ee-Morvan D., Groussin O. et al., 2013, A&A 557, A88
- Colangeli L., Bussoletti E., Cecchi Pestellini C. et al., 1998, Icarus 134, 35
- Combi M.R., Makinen J.T.T., Bertaux J.-L. et al., 2013, Icarus 225, 740
- Das H.S., Medhi B.J., Wolf S. et al., 2013, MNRAS 436, 3500
- DiSanti M.A., Villanueva G.L., Paganini L. et al., 2014, Icarus 228, 167
- Dones L., Weissman P.R., Levison H.F., Duncan M.J., 2004, in "Comets II", M. Festou, H.U. Keller & H.A. Weaver Eds., Univ. Arizona Press, Tucson
- Duncan M., Quinn T., Tremaine S., 1987, AJ 94, 1330
- Farnham T.L., 2009, Planet. Space Sci. 57, 1192
- Feaga L.M., A'Hearn M.F., Farnham T.L. et al., 2014, AJ 147, 24
- Fink U. & Rubin M., 2012, Icarus 221, 721

- Fulle M., 1999, Planet. Space Sci. 47, 827
- Fulle M., Mikuz H. & Bosio S., 1997, A&A 324, 1197
- Fulle M., Cremonese G. & Bohm C., 1998, AJ 116, 1470
- Gehrz R.D. & Ney E.P., 1992, Icarus 100, 162
- Gicquel A., Milam S.N., Coulson I.M. et al., 2015, ApJ 807, 19
- Hadamcik E., Sen A.K., Levasseur-Regourd A.C. et al., 2014, Met. & Planet. Science, 49, 1, 36
- Holmberg J., Flynn C. & Portinari L., 2006, MNRAS 367, 449
- Ivanova O.V., Skorov Y.V., Korsun P.P., Afanasiev V.L., Blum J., 2011, Icarus 211, 559
- Ivanova O.V., Borisenko S.A., Andreev M.V., 2014, So.Sys.Res. 48, 375
- Ivanova O.V., Neslušan L., Krišandová Z.S., Svoreň J., Korsun P.P. et al., 2015, Icarus 258, 28
- Jewitt D.C., 2009, AJ 137, 4296
- Kelley M.S., Fernández Y.R., Licandro J. et al., 2013, Icarus 225, 475
- Korsun P.P. & Chorny G.F., 2003, A&A 410, 1029
- Korsun P.P., Kulyk I.V., Ivanova O.V. et al., 2010, Icarus 210, 916
- Korsun P.P., Rousselot P., Kulyk I.V., Afanasiev V.L., Ivanova O.V., 2014, Icarus 232, 88
- Lamy P., Toth I., Fernandez Y.R. & Weaver H.A., 2004, in Comets II, eds. M. Festou, H.U. Keller & H.A. Weaver (Tucson:Univ. Arizona Press)
- Lamy P. Toth I., Weaver H.A., A'Hearn M.F. & Jorda L., 2009, A&A 508, 1045
- Landolt A.U., 1992, AJ 104, 1, 340
- Lara L.-M., Licandro J., Tozzi G.P., 2003, A&A 404, 373
- Lara L.-M., Tozzi G.P, Boehnhardt H., Di Martino M., Schulz R., 2004, A&A 422, 717
- Levison H.F., Duncan M.J., Brasser R., Kaufmann D.E., 2010, Science 329, 187
- Lowry S. C., Fitzsimmons A., 2001, A&A, 365, 204
- Lowry S. C., Fitzsimmons A., 2005, MNRAS, 358, 641
- Lowry S. C., Fitzsimmons A., Cartwright I. M., Williams I. P., 1999, A&A, 349, 649
- Lowry S. C., Fitzsimmons A., Collander-Brown S., 2003, A&A, 397, 329
- Mazets E.P., Aptekar R.L., Golentskii S.V. et al., 1986, Nature 321, 15, 276
- Mazzotta Epifani E. & Palumbo P., 2011, A&A 525, A62
- Mazzotta Epifani E., Palumbo P., Capria M.T. et al., 2006, A&A 460, 935
- Mazzotta Epifani E., Palumbo P., Capria M.T. et al., 2007, MNRAS 381, 713
- Mazzotta Epifani E., Palumbo P., Capria M.T. et al., 2008, MNRAS 390, 265
- Mazzotta Epifani E., Palumbo P., Capria M.T. et al., 2009, A&A 502, 355
- Mazzotta Epifani E., Dall'Ora M., Di Fabrizio L. et al., 2010, A&A 513, A33
- Mazzotta Epifani E., Dall'Ora M., Perna D., Palumbo P., Colangeli L., 2011, MNRAS 415, 3097
- Mazzotta Epifani E., Perna D., Di Fabrizio L. et al., 2014a, A&A 561, A6
- Mazzotta Epifani E., Perna D., Licandro J., 2014b, A&A 565, A69
- Meech K.J., Pittichova K.J., Bar-Nun A. et al., 2009, Icarus 201, 719
- Paganini L., Mumma M.J., Villanueva G.L. et al., 2012, ApJL 748, L13
- Price M.C., Kearsley A.T., Burchell M.J. et al., 2010, Meteoritics & Pla. Sciences 45, 9, 1409
- Russell H.N., 1916, ApJ 43, 173
- Schleicher, D. G. 2007, Icarus, 190, 406
- Schleicher, D. G., Millis, R. L., & Birch, P. V. 1998, Icarus, 132, 397
- Shubina O., Kulyk I., Korsin P., Romanjuk Ya., 2014, Adv. in Astron. & Spa. Phys., 4, 38
- Sitko M.L., Russell R.W., Woodward C.E. et al., 2013, 44th LPSC, March 18-22, The Woodlands, Texas. LPI Contrib. No. 1719
- Solontoi M., Ivezic Z., Juric M. et al., 2012, Icarus 218, 571
- Snodgrass C. Fitzsimmons A. & Lowry S., 2005, A&A 444, 287
- Szabó G.M., Kiss L.L., Sárneczky K., Sziládi K., 2002, A&A 384, 702
- Tozzi G.P., Boehnhardt H., Lo Curto G., 2003, A&A 398, L41
- Villanueva G.L., Mumma M.J., DiSanti M.A. et al., 2012, Icarus 220, 291
- Zubko E., Videen G., Hines D.C. et al., 2015, Planet. Spa. Sciences 118, 138

Highlights

- Very active and "dusty" comet, even at $r_h \sim 6$ AU
- Complex coma morphology, with jet-like structures and spiralling outflows.
- Measured dust loss rate Q_d among the highest for minor bodies at small r_h (< 3 AU)